Supporting Information

In-Doped ZnO Nanofibers with Acharia stimulea-inspired Morphology: A Promising Sensing Platform for Highly Rapid and Sensitive Detection of Listeria Biomarker 3-Hydroxy-2-Butanone

*Jing-Wen Liu [a], Gang-Long Song [a], Xiao-Xue Lian [a], Zhuang-Zhuang Qu [b], Yan Li [a, *]*

[a] College of Science, Civil Aviation University of China, Tianjin, 300300, PR China

[b] School of Energy and Constructional Engineering, Shandong Huayu University of Technology, Dezhou, 253000, Shandong, PR China

**Corresponding author: Yan Li, liyan01898@163.com, (086)-022-24092514*

Co-first authors: Jing-Wen Liu and Gang-Long Song have contributed equally to this work.

Text S1. Material characterization methods

Necessary techniques were utilized to characterize the as-prepared samples. Mineral composition and crystal structure of all samples were carefully investigated using DX-2000 X-ray diffractometer (XRD, target mater ial is Cu, λ = 0.154184 nm, tube voltage and tube current are 30 kV and 25 mA respectively, scanning speed was 0.01 deg./s, scanning range is 30°-70°). Microstructure and morphology were studied using a transmission electron microscopy (TEM, FEI Tal os F200X, the acceleration voltage is 200 kV, point resolution is 0.25 nm) and a scanning electron microscopy (SEM, TESCAN MIRA LMS, the resolution of the secondary electron image is 0.9 nm, and the resolution of the backscattered electron image is 2 nm. The acceleration voltage is 200 V-30 kV and the probe beam current is 1 pA-100 nA). Chemical constituents were analyzed using Thermo escalab 250XI (XPS, the excitation source is Al Kα ray (hν = 1486.6 eV), the beam spot is 650 μm, the power is 150W, the acceleration voltage is 14.8 kV, and the filament current is 1.6 A. Charge correction was performed using contaminated carbon C1s = 284.8 eV) and energy dispersion X-ray energy spectrometry (EDS, JED-2300T). The pore structure and specific surface area of the materials were characterized by JW-BK200C. The optical band gap width of the sample was tested using an ultraviolet-visible landscape photometer (UV-2600).

Text S2. Gas sensor testing

Gas-sensing measurements were performed using a CGS-8 gas sensing analysis system (Beijing Elite Technology Co.). The sensor under test was placed in a cylindrical test chamber, and it was equipped with a temperature-controlled heating stage to adjust the different operating temperatures. All gas-sensing measurements were conducted under a relative humidity condition of 30% RH. For humidity-specific tests on the gas-sensing devices, an air humidifier was used to precisely set and maintain the required humidity levels within the chamber. In addition, a syringe was used to inject a precise volume of volatile gases into the chamber through a rubber septum. The concentration of gases in the test chamber was calculated using Eq. (1) [1, 2]:

$$C = 22.4 \times \varphi \times \rho \times V_1 \times {}^{1000}/_{(M \times V_2)} \quad (1)$$

Where C (ppm) is the target gas concentration, φ is expressed as the purity of the liquid

(%), ρ (g/mL) is the liquid density of the target gas, V1 (μL) is the fluid volume of the target gas, M (g/mol) is the molecular weight of the target gas and V2 (L) is the volume of the chamber. The response (R) of the sensors was calculated on the basis of the relative change in sensor resistance from air (R_a) to target gas (R_g), using the following formula [3]:

$$R = R_a/R_g \tag{2}$$

Moreover, the response (τ_{res}) and recovery times (τ_{rec}) were determined as the time taken to reach 90% of the final equilibrium value.

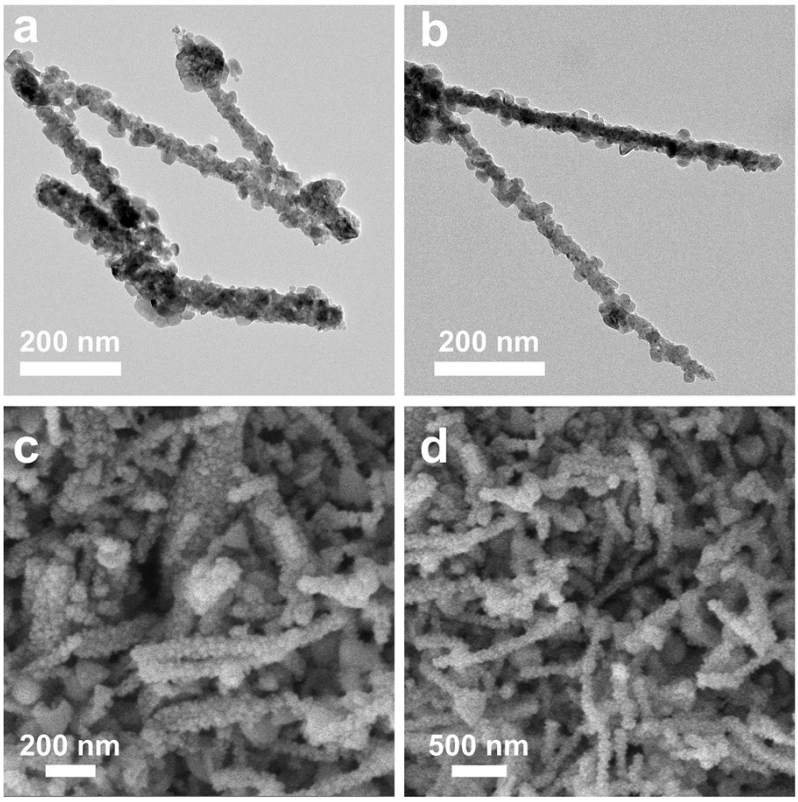

Fig. S1. (a-b) SEM and (c-d) HRTEM images of the IZ4 nanofibers.

LOD calculation:

According to literature reports, the calculation equation for the theoretical detection limit (LOD) is typically used and is shown below [4]:

$$LOD\ (ppm) = 3 \times \frac{S_{noise}}{b} \tag{3}$$

In Eq. (3), b is the slope value obtained by linearly fitting the response value and 3H-2B concentration curve. Take N = 10 data points (Y_i) from the baseline of response versus time curves before 3H-2B exposure (Fig. S2). Then, calculate the regular residual (Y_i-Y) of the polynomial fit and determine the root-mean-squared deviation (S_{noise}) using Eq. (4) and Eq. (5) [5]. Here, Y_i represents the measured data point and Y represents the corresponding value calculated from the curve-fitting equation (see Table S1):

$$V_x^2 = \sum_{i=1}^{N} (Y_i - Y)^2 \tag{4}$$

$$S_{noise} = \sqrt{\frac{V_x^2}{N-1}} \tag{5}$$

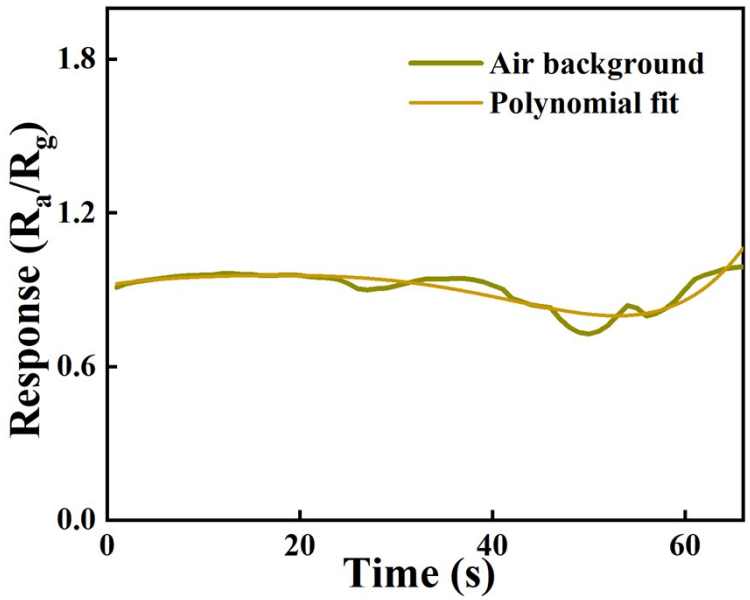

Fig. S2. The 5th order polynomial fitted response of the 3% In-ZnO sensor versus time at the baseline before 3H-2B exposure.

Table S1. 5th order polynomial fitting data for the 3% In-ZnO sensor.

Times of measurement	Y_i	Y	(Y_i-Y)	$(Y_i-Y)^2$
1	0.9468	0.9027	0.0441	1.9448E-3
2	0.9411	0.9044	0.0367	1.3469E-3
3	0.9004	0.9445	-0.0441	1.9448E-3
4	0.8857	0.9372	-0.0515	2.6522E-3
5	0.8121	0.7385	0.0736	5.4169E-3
6	0.8008	0.9493	-0.1485	2.2052E-2
7	0.7991	0.8432	-0.0441	1.9448E-3
8	0.8574	0.8942	-0.0368	1.3542E-3
9	0.8783	0.9372	-0.0589	3.4692E-3
10	1.040	0.9887	0.0513	2.6317E-3

Table S2. Calculation of slope, S_{noise} and LOD.

Sensing Material	b (ppm^{-1})	V_x^2	S_{noise}	LOD (ppm)
3% In-ZnO	8.0619	4.4758E-2	7.05E-2	0.0262

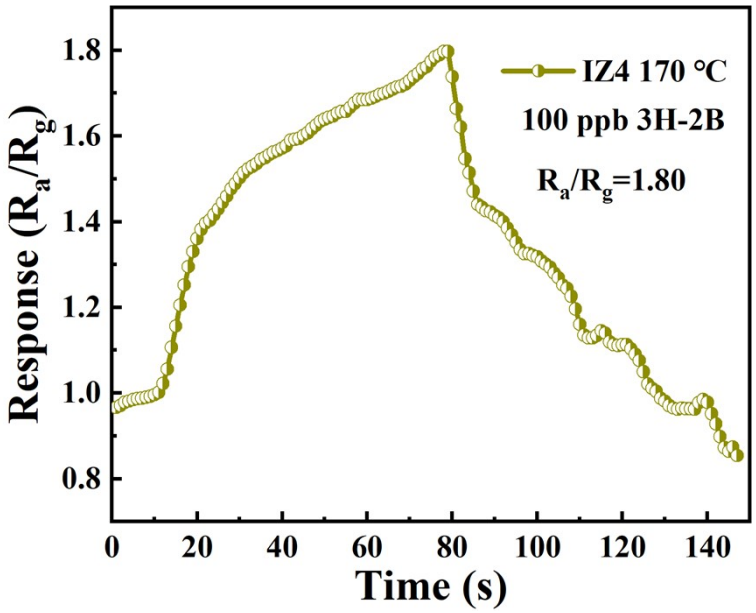

Fig. S3. Response curve of the IZ4 sensor toward 100 ppb 3H-2B.

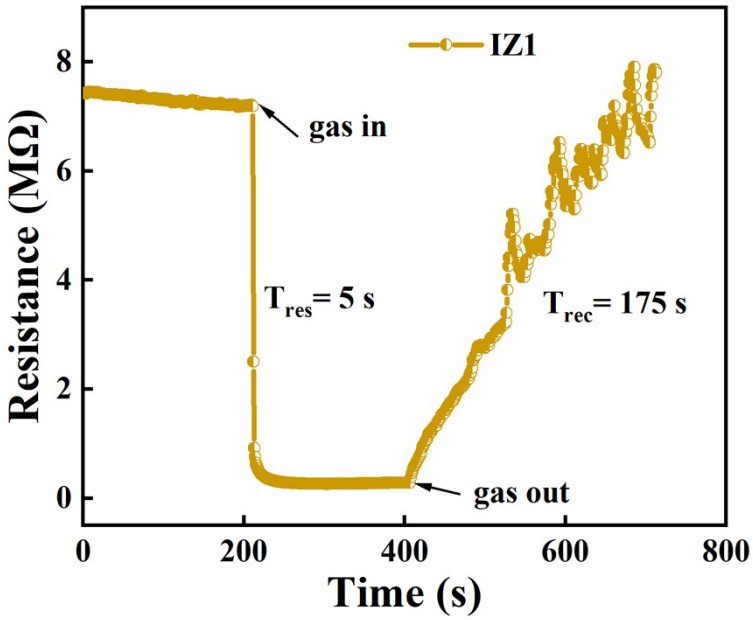

Fig. S4. Response-recovery time curves of the IZ1 sensor toward 100 ppm 3H-2B.

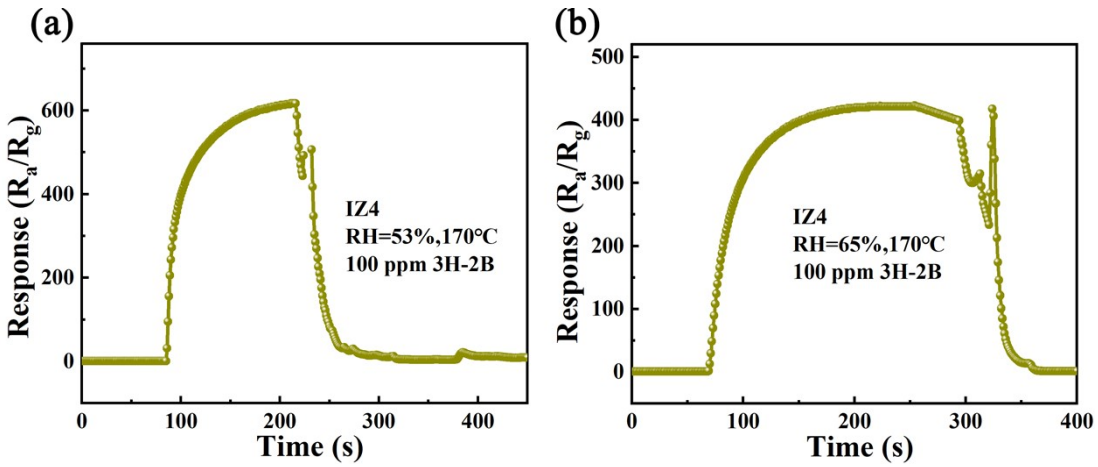

Fig. S5. Dynamic response-recovery curves of the IZ4 sensor toward 100 ppm 3H-2B at RH values of 53% and 65%

References

[1] Y. Luo, A. Ly, D. Lahem, J.D.M. Martin, A.-C. Romain, C. Zhang, M. Debliquy, Role of cobalt in Co-ZnO nanoflower gas sensors for the detection of low concentrati on of VOCs, Sensors and Actuators B: Chemical, 360 (2022). https://doi.org/10.1016/j.snb.2022.131674.

[2] C. Sun, J. Shao, G. Pan, X. Yang, Triethylamine gas sensor based on Zn_2SnO_4 po lyhedron decorated with Au nanoparticles and density functional theory investigation, S ensors and Actuators B: Chemical, 408 (2024). https://doi.org/10.1016/j.snb.2024.135510

[3] Y. Zhang, M. Wang, X. San, L. Zhang, N. Wang, G. Wang, D. Meng, Y. Shen, Highly selective gas sensors for formaldehyde detection based on ZnO@ZIF-8 core-she ll heterostructures, Sensors and Actuators B: Chemical, 398 (2024). https://doi.org/10.10 16/j.snb.2023.134689.

[4] X. Shao, D. Zhang, M. Tang, H. Zhang, Z. Wang, P. Jia, J. Zhai, Amorphous Ag catalytic layer-SnO_2 sensitive layer-graphite carbon nitride electron supply layer synerg y-enhanced hydrogen gas sensor, Chemical Engineering Journal, 495 (2024). https://doi.org/10.1016/j.cej.2024.153676.

[5] T. Murugesan, R.R. Kumar, A. Ranjan, M.-Y. Lu, H.-N. Lin, Fabrication of large-area Au nanoparticle decorated ZnO@ZIF-8 core-shell heterostructure nanorods for ppb -level NO_2 gas sensing at room temperature, Sensors and Actuators B: Chemical, 402 (2024). https://doi.org/10.1016/j.snb.2023.135106.